Oral Presentation

The 7th TSME International Conference on Mechanical Engineering
13-16 December 2016

TSME ICOME 2016
Mechanical Engineering Innovation for Green Society

TSF0008

Structural Change in Surfactant Solutions in Large Amplitude Oscillation Shear Flow

Takashi Koshiba[1,*] and Takehiro Yamamoto[2]

[1] National Institute of Technology, Nara College, 22 Yatacho, Yamatokoriyama, Nara, 639-1080, Japan
[2] Osaka Electro-Communication University, 18-8, Hatsu-cho, Neyagawa, Osaka, 572-8530, Japan
[*] Corresponding Author: koshiba@mech.nara-k.ac.jp, TEL: +81-743-55-6082, FAX: +81-743-55-6089

Abstract

In the present study, the structural change in wormlike micelles solution in large amplitude oscillating shear flow was examined. The oscillating flow was produced by two parallel plates, and the experiments were carried out focusing on the white turbidity, which represents the change in micellar structure. Test fluid was provided an aqueous solution of CTAB/NaSal system. From flow visualization, we confirmed that remarkable white turbidity occurred immediately after the startup of flow. In measurement of the scattering intensity of light using a laser light, it was found that the signal of scattering intensity could capture the occurrence of white turbidity, and that the behavior suggesting the orientation of wormlike micelles appeared at the switching of flow direction in the oscillational shear flow. Furthermore, it was confirmed that the signal analysis using the wavelet transformation could show the characteristic in regard to the change in micellar structure in oscillational shear flow.

Keywords: Surfactant solution, Oscillation shear flow, Micellar structure, Structural change, White turbidity

1. Introduction

Surfactant molecule is constructed by the coupling of hydrophobic and hydrophilic groups. Surfactant solutions have been used in many industrial fields. One of the characteristic features of surfactants is the formation of aggregates called micelles in solution [1]-[3]. The formation of micelles needs surfactants with the concentration above a critical micellar concentration and is enhanced by an addition of salt. The configuration of micelles depends on the concentration of surfactants and added salts. Especially, in concentrated solutions, wormlike micelles are formed in the solutions. The flow of wormlike micellar solutions exhibits remarkable viscoelasticity like polymer solutions. However, in this case, there are various interesting phenomena that do not appear in polymer cases. One of them is the shear thickening property appearing in steady shear viscosity curve; that is the increment of shear viscosity increasing in shear rate [4]. This phenomenon is related to the structural change in micelles induced by shear flow and has received remarkable attention in rheology. Consequently, there are many reports discussing the relation between the micellar structure and flow behavior [5]-[7]. In these reports, the micellar structure is mainly evaluated by the frequency-dependent storage modulus G' and loss modulus G'', which are measured by the linear viscoelastic experiments. Meanwhile, the structural change in micelles induced by a flow appears in a non-linear flow field and its behavior can be confirmed as the cloudiness of fluid occurring in flowing, that is the white turbidity. In general, the linear viscoelasticity is measured by applying a small amplitude oscillating flow to the test fluid, while the experiment of non-linear viscoelasticity is conducted with a simple shear flow using a rotational rheometer or a pipe flow. However, in order to examine the microstructure of micelles in non-linear flow field, the experiments with the large amplitude oscillating shear flow (LAOS) has been performed by various researchers, recently [8]-[10]. On the large amplitude shear flow, because both the deformation given in fluids and time scale in structural change can be controlled independently, it is considered that the additional information to micellar structure might be obtained. Furthermore, the LAOS experiments are applied to other complex fluids as well as surfactant solution, and those results provide the useful information with respect to the microstructure of complex fluid like suspensions and emulsions.

With such a background, we carried out the experiments of large amplitude oscillating flow for surfactant solution to examine the occurrence of white turbidity representing the structural change in micelles. Normally, the oscillating regime in the LAOS experiments has been produced by the sinusoidal motion. However, in the present experiment, a periodical triangle wave with constant amplitude was used to make an oscillational flow. In the case of triangle wave, since the state of flow is in a constant speed and its direction is switched every a half period, the test fluid becomes to be subjected to a constant shear deformation. Especially, since the shear deformation at a switching of flow direction is in a step state, it is considered that a periodical transient change in shear rate is convenient for the examination of the transient response of white turbidity that can visualize the structural change in micelles. Then, we mainly carried out the experiments with regard to the observation and evaluation of white turbidity in a flow of surfactant solution and discussed structural changes.

2. Experimental

2.1 Experimental apparatus and method

Figure 1 shows the schematic view of experimental apparatus. Large amplitude oscillational shear flow in this experiment is based on the Couette flow between two parallel plates and is produced by a linear driving unit. The driving unit is constructed by a rack-and-pinion gear with two limit switches. The moving speed of rack is constant and is controlled by the rotational speed of induction motor. The displacement of rack in moving is monitored by the optical displacement sensor. In this experiment, two kinds of experiments were carried out. One is the flow visualization in oscillating flow and the other is the measurement of scattering intensity of light transmitting a shear flow of surfactant solution. The schema of each measuring unit is shown in Fig.1.

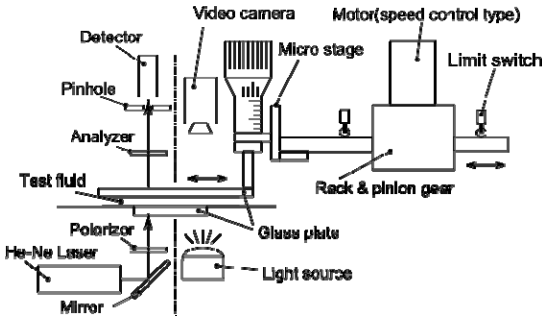

Fig.1 Schematic view of experimental apparatus.

Figure 2 is the detail of test section. The depth of container is 56 mm. Firstly, small amount of test fluid was set in a container. Next, contacting glass plate on fluid surface, we achieved the experimental preparation by setting the gap between two glass plates to 0.5 mm. The oscillational flow is produced by a reciprocal movement of the upper glass plate. In order to observe shear flow, the other glass plate was embedded in the bottom of container.

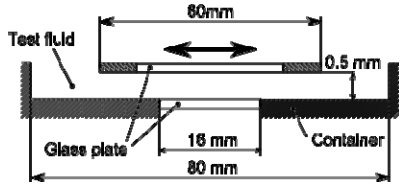

Fig.2 Details of test section.

The experimental conditions are shown in Table 1. In the present study, the period of oscillation is selected as the experimental parameter. Consequently, the fluid is subjected to a constant strain, which magnitude is 24, and the shear rate varies in the range from 18 to 44 s^{-1}. In general, in the linear viscoelasticity experiment using the small amplitude oscillating shear flow, the magnitude of shear strain is less than 1.

Table 1 Experimental Conditions

Conditions	Stroke (mm)	Period (sec.)	Apparent shear rate (1/s)
A	12	3.0	18
B	12	1.8	30
C	12	1.3	44

The shear rate in this experiment was evaluated as the apparent value using Eq.(1),

$$\Gamma_{app} = \frac{V}{h} \tag{1}$$

where h is the gap between the two glass plates and its magnitude is 0.5 mm. V is the velocity of glass plate.

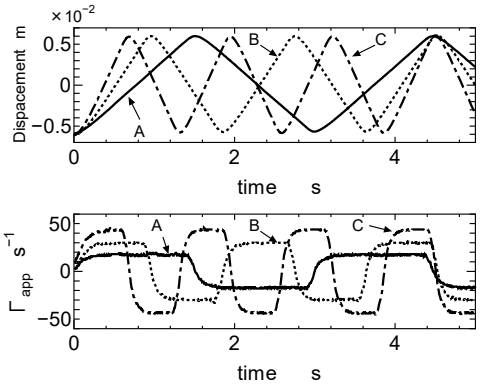

Fig.3 Time change in the displacement of glass plate, and in the apparent shear rate.

Figure 3 shows the time change in the displacement of glass plate, and in the apparent shear rate. In Fig.3, we can confirm that the movement of glass plate obeys triangle wave, and that the apparent shear rate forms approximately square waves. However, at switching the flow direction, the time delay in shear rate occurs.

2.2 Test fluid

With respect to test fluid, we used CTAB (cetyltrimethylammonium bromide) as surfactant, and NaSal (sodium salicylate) as additive salt. Solvent is the distilled water using in a liquid chromatography. The concentration of CTAB is 0.03 mol/l, the ratio of NaSal concentration relative to CTAB is 4.0. The rheological characteristics of surfactant solution with this ratio were well known as the fluids having remarkable viscoelastic properties. Figure 4 shows its linear viscoelastic properties. Furthermore, it is known that the linear properties of CTAB/NaSal is consistent with a single mode of Maxwell type model (Eq.(2)) which is a fundamental model for linear viscoelasticity of complex fluids.

$$G' = \frac{G_0(\omega\tau_m)^2}{1+(\omega\tau_m)^2}, \quad G'' = \frac{G_0\omega\tau_m}{1+(\omega\tau_m)^2} \qquad (2)$$

where G_0 is the plateau modulus and τ_m the relaxation time. In the comparison of linear viscoelasticity for test fluid with those of the Maxell model, we obtained that the value of G_0 is 3.0 Pa and τ_m is 1.55 s.

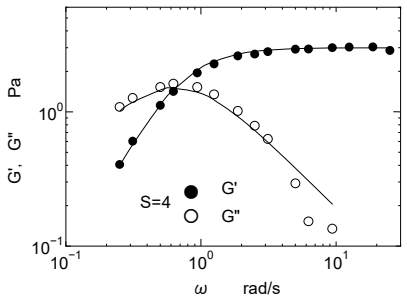

Fig.4 Linear viscoelastic properties of test fluid.

Figure 5 shows the steady shear properties of the test fluid. We find that the curve of steady shear viscosity has non-linearity where the shear viscosity decreases with the increment of shear rate as a whole. Furthermore, the difference of the first normal stress, which means an elasticity of fluid, increases with the increase in shear rate. However, in the curve of shear viscosity in Fig.5, the inclination of shear viscosity becomes gentle around the shear rate $\dot{\gamma}$ of 10 s^{-1}. This change in shear viscosity has been reported in other reports using the same fluid as the present experiment. In these reports, it has been shown that the shear-thickening property in shear viscosity occurs in the neighborhood of shear rate $\dot{\gamma} = 10$ s^{-1}. Although the results in Fig.4 was less pronounced, it is considered that the slight change in shear viscosity in Fig.4 suggests the transition from the shear thinning of shear viscosity to the shear thickening property. Besides, in the flow condition at $\dot{\gamma} > 10$ s^{-1}, it is predicted that the structural change in micelles might affect to a flow state.

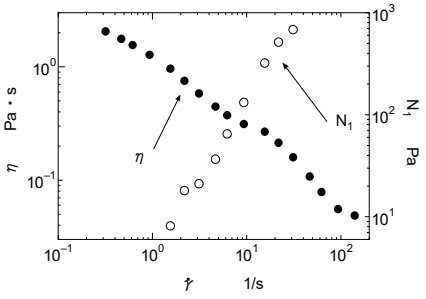

Fig.5 Steady shear properties of test fluid.

3. Results and discussion

3.1 Observation of white turbidity

Figure 6 shows the results of flow visualization with respect to oscillating shear flow at the shear rate of 30 s^{-1}. The image of Fig.6(b) shows a state just after the onset of flow, and (c) is the images at the switching of flow direction after several cycles. In comparison with Fig.6(a), which is in a rest state, we can find that the image of Fg.6(b) is cloudy in white over the visualizing region, and the streak pattern partially appears in parallel to the flow direction. However, the degree of white turbidity became thin with the increment of oscillating cycle (Fig.6(c)). Besides, by the contrast of light and shade in the image, the streak pattern occurs more pronounced. According to previous reports [11]-[12], it is considered that the occurrence of white turbidity means the structural change in micelles induced by flow, and the cause relates to the change in birefringence due to the breakup of wormlike micelles. Besides, it is thought that the streak pattern seen in the image of white turbidity is caused by the effect of the irregularity of micellar concentration. Consequently, since the results in Fig.6 have many common characteristics to the previous results, it is found that the change in micellar structure occurs in the flow regime like a linear movement.

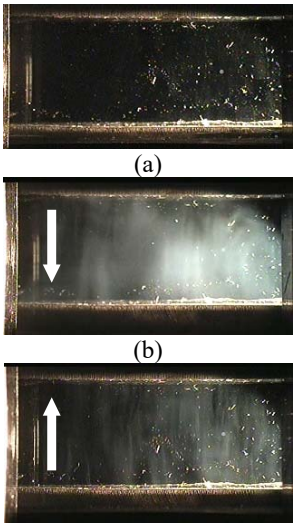

Fig.6 Captured images in the oscillational shear flow at the shear rate of 30.0s^{-1}. The arrows in the figure indicate the moving direction of glass plate.
(a) at rest, (b) and (c) at the shear rate of 30 s^{-1}

In general, it is known that the micellar solution has a self-assembled structure. Although in the micellar solution the change in micellar structure is induced by flow, the structural change returns to the original state with time after the cessation of flow. At that time, the time scale retuning to the original state is

closely related to the relaxation time of fluid. Therefore, the difference of the white turbidity between Fig.6(b) and (c) might be affected by the relaxation mechanism of micellar solution.

3.2 Time change in the intensity of scattering light

For the sake of evaluation of the white turbidity, we measured the scattering intensity of light using a He-Ne laser. The incident position of laser light is the center of test section and the incident direction of light is from bottom to top. After transmitting two polarizing plates in the crossed-nichol state, the intensity of scattering light was detected by the photodiode. Figure 7 shows the results at each experimental condition A-C. Besides, for the sake of facilitating the comparison between the oscillating flow and the intensity of light, the displacement of rack is included in Fig.7. The intensity of light is normalized by the maximum value of light intensity in measuring.

From Fig.7, we can find that the change in scattering intensity of light at startup of flow becomes remarkable in each condition. Especially, the time range showing the high intensity maintains before the first switching of a flow direction. After that, however, the peak of light intensity decreases with time, and its occurrence is limited to the short period at the time of switching of flow direction. In addition, the value of $I(t)/I_{max}$ between the peaks of intensity curve becomes to be almost zero. With regard to this, the scattering direction of light means random. This fact suggests that there is the time lag until orienting wormlike micelles to a flow direction. Furthermore, we can find the results like corroborating such phenomenon at the startup of flow; that is the time y of scattering intensity.

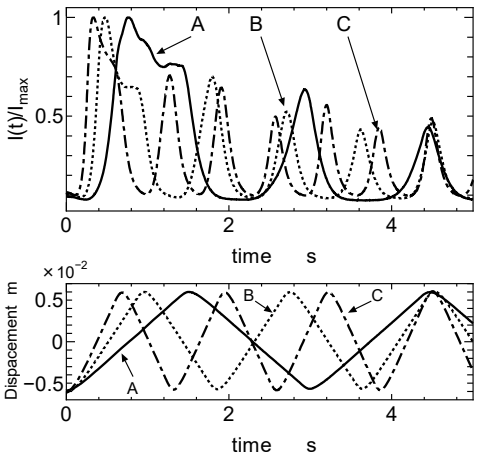

Fig.7 Time change in the scattering intensity of a He-Ne laser light transmitting an oscillational flow.

As the whole, such characteristics with respect to a scattering intensity were consistent with those photographed by the digital video camera. Consequently, the results in Fig.7 are considered to quantitatively capture the occurrence of white turbidity shown in Fig.6.

3.3 Signal analysis using the Wavelet transformation

In order to examine the details of signal with respect to the scattering intensity of light, we used the wavelet transformation [13]. The definition of wavelet transformation W is shown in Eqs.(3)-(5). The function $f(t)$ means the analyzed signal, and $\psi(t')$ means the mother wavelet. In this analysis, the Morlet wavelet was used as the mother wavelet [14].

$$W(a,b) = \left\langle f(t), \psi_{a,b}(t) \right\rangle = \frac{1}{\sqrt{a}} \int_{-\infty}^{\infty} f(t)\psi(t')dt \quad (3)$$

$$\psi(t') = \frac{1}{\sqrt{2\pi\sigma^2}} e^{\left(-t'^2/(2\sigma^2)\right)} e^{i\omega t} \quad (4)$$

$$t' = \frac{t-b}{a} \quad (5)$$

where a is the scale factor that represents the dilation of wavelet and b the shift factor that relates to the movement of wavelet. Besides, σ and ω are the independent variables which relate to the base wavelet. Figure 8 shows the effect of a and b to the wavelet function. In Fig.8, we can confirm the effect of two factors by the deformation of a wave shape.

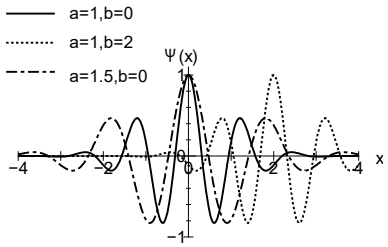

Fig.8 Effect of a scale factor a and a shift factor b on the mother wavelet function.

Figure 9 shows the results of the wavelet transformation in regard to the flow condition A (the shear rate of 18 s^{-1}). In Fig.9, the color display means the distribution of wavelet coefficient normalized by maximum value, i.e the white part is 1 and the black 0. Also, the analyzed signal is shown in comparison with wavelet coefficients. In the present experiment, the range of scale factor is from 1 to 256. The value of a scale factor corresponds to the frequency characteristic of analyzed signal. When the value of a scale factor is high, the frequency resolution becomes high, while in the case of low scale factor, the frequency resolution becomes low.

TSF0008

From Fig.9, considering the periodicity of analyzed signal, we find that the distribution of coefficient after 4 s from a startup of flow is very similar and the peaks of coefficient are located at the scale factor of about 110. However, the distribution of wavelet coefficient after the startup of flow spreads over a wide range of scale factor. Due to this result, it is predicted that the structural change in micelles occurs during a long time.

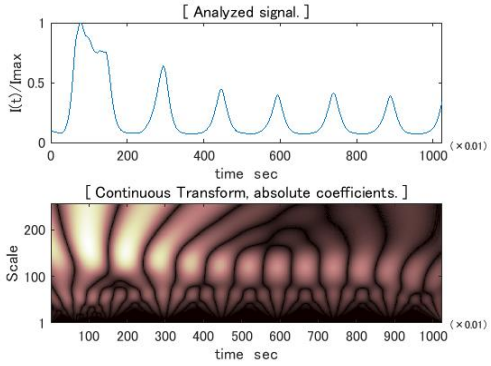

Fig.9 Wavelet analysis with respect to the scattering signal of transmitting light at the flow condition A.

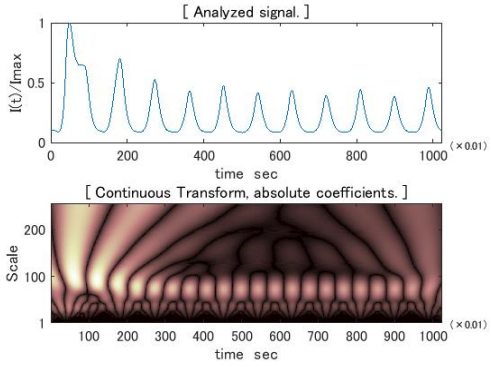

Fig.10 Wavelet analysis with respect to the scattering signal of transmitting light at the flow condition B.

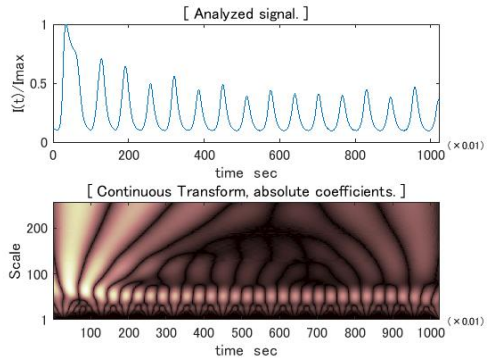

Fig.11 Wavelet analysis with respect to the scattering signal of transmitting light at the flow condition C.

Figure 10 and 11 show the results of wavelet transformation at the flow conditions B and C. In each figure, the tendency in distribution of wavelet coefficient is similar to that in Fig.9. However, in comparison with the peak of analyzed signal curve, we can find that the distribution of coefficient becomes finer, and that the value of scale factor is lower than that of Fig.9. In addition, it is found that the difference in expansion of the scale factor at the startup of flow is not remarkable.

4. Conclusion

In this experiment, the structural change in micelles of surfactant solution in large amplitude oscillating shear flow was examined. We discussed on the occurrence of white turbidity which represents the structural change in micelles. From the flow visualization, it was found that the occurrence of white turbidity remarkably occurred at the switching of flow direction. In the measurement of scattering intensity of light using a laser light, the scattering signal curve was linked with the behavior of the occurrence of white turbidity. Furthermore, examining the scattering signal with the wavelet transformation, we confirmed that the occurrence of white turbidity could be characterized by the distribution of wavelet coefficient.

References

[1] Shikata, T., Hirata, H., and Kotaka, T., Micelle Formation of Detergent Molecules in Aqueous Media: Viscoelastic Properties of Aqueous Cethyltrimethylammonium Bromide Solutions, *Langmuir*, vol.3, 1987, pp.1081-1086.

[2] Shikata, T., Hirata, H., and Kotaka, T., Micelle Formation of Detergent Molecules in Aqueous Media. 2. Role of Free Salicylate Ions on Viscoelastic Properties of Aqueous Cetyltrimethylammonium Bromide-Sodium Salycylate Solutions, *Langmuir*, vol.4, 1988, pp.354-359.

[3] Shikata, T., Viscoelastic Behavior of Aqueous Surfactant Micellar Solution, *Nihon Reoroji Gakkaishi*, vol.31(1), 2003, pp.23-32.

[4] Liu, C.H., Pine, D.J., Shear-Induced Gelation and Fracture in Micellar Solution, *Phys. Rev. Lett*, vol.77(10), 1996, pp.2121-2124.

[5] Kadoma, I.A., Ylitao, C., and Egmond, J.W., Structural transitions in wormlike micelles, *Rheol Acta*, vol.36, 1997, pp.1-2.

[6] Kim, W.J., Y, S.M., Effects of Sodium Salicylate on the Microstructure of an Aqueous Micellar Solution and its Rheological Responses, *J. Colloid Interface Sci.*, vol.232, 2000, pp.225-234.

[7] Ouchi, M., Takahashi, T., and Shirakashi, M., Flow-Induced Structure Change and Flow-Instability of CTAB/NaSal Aqueous Solution in a Two-Dimensional Abrupt Contraction Channel, *Nihon Reoroji Gakkaishi*, vol.34(4), 2006, pp.229-234.

[8] Hyun, K., Kim, S.H., Ahn, K.H., and Lee, S.J., Large amplitude oscillatory shear as a way to classify the complex fluids, *J Non-Newtonian Fluid Mech*, vol.107, 2002, pp.51-65.
[9] Dimitriou, C.J., Casanellas, L., Ober, T.J., and McKinley, G.H., Rheo-PIV of a shear-banding wormlike micellar solution under large amplitude oscillatory shear, *Rhol Acta*, vol.51, 2012, pp.395-411.
[10] Kim, S., Mewis, J., Clasen, C., and Vermant, J., Superposition rheometory of a wormlike micellar fluid, *Rheol Acta*, vol.52, 2013, pp.727-740.
[11] Takahashi, T., Yako N., and Shirakashi, M., Relationship between Shear-Induced Structure and Optical Anisotoropy on CPyCl/NaSal Aqueous Solution, *Nihon Reoroji Gakkaishi*, vol.29(1), 2001, pp.27-32.
[12] Yamashita, A., Mori, K., Sawa, K., and Yamamoto T., Creep Tests, Flow Birefringence Measurement, and Flow Visualization of Aqueous Solutions of CTAB and NaSal in Shear Flow between Parallel Olates, *J. Fluid Sci. Tech.*, vol.4(3), 2009, pp.699-710.
[13] Munoz, A., Ertle, A., and Unser, M., Continus wavelet transform with arbitrary scales and O(N) complexity, *Signal Processing*, vol. 82, 2002, pp.749-757.
[14] Bussow, R., An algorithm for the continuous Morlet wavelet transform, *Mechanical Systems and Signal Processing*, vol.21, 2007, pp.2970-2979.